Metal emission lines as diagnostic tools for shock waves in outer atmospheres of M-type Mira stars

He. Richter and E. Sedlmayr
(Zentrum für Astronomie und Astrophysik, TU Berlin, D-10623 Berlin, Germany)
P.R. Wood
(Research School of Astronomy and Astrophysics, Australian National University, ACT 2611, Australia)
Correspondence to: richter@astro.physik.tu-berlin.de

1. Introduction

One way to reveal the thermo- and hydrodynamical conditions in M-type Mira atmospheres is to study the various emission lines which are emitted behind a shock front and can be observed over a substantial portion of the pulsation period. Analyzing a time-resolved series of these emission lines offers the possibility to determine these conditions in different atmospheric layers influenced by the passing shock wave. In particular, the metal emission lines are a diagnostic tool to probe the hydrodynamical conditions of the outer, dust-forming layers of the atmosphere, because they appear late in the pulsation cycle when the shock wave has reached these layers.

We present quantitive data on radial velocities, shapes, widths, and fluxes of metal emission lines obtained by spectral observations in the optical wavelength region for a sample of six M-type Miras (periods 281 - 389 days), namely R Aql, RR Sco, R Car, R Leo, S Scl, and R Hya (cf. Richter & Wood 2001). Because of the multiple phase coverage of our observations, the data show the history of the shock as it emerges through the deep photosphere and then moves outward through the atmosphere.

2. Observation

- **Instruments:**
  1.88 m telescope at Mount Stromlo Observatory, Coudé Echelle spectrograph, 81 cm camera, 2 x 4k Site CCD detector

- **Resolutions:**
  Maximum resolution observ. (300 μm slit): 4.6 $\frac{km}{s}$
  Spectophotometric observ. (1500 μm slit): 15.3 $\frac{km}{s}$

- **Julian dates and phases:**

JD[a]	Phase					
	RR Sco	R Aql	R Car	R Leo	S Scl	R Hya
	P[b]: 281	284	309	310	363	389
1153	-	-	-0.16	-	-	-
1169	-	-	-	-	0.02	-
1206	-	-	-0.09	0.43	-	-
1268	-	0.01	0.11	0.63	-	-
1357	0.29	0.32	0.39	-	0.52	0.08
1375	-	0.39	0.45	-	0.58	0.12
1412	0.48	0.50	0.57	-	0.67	0.21
1440	0.58	-	0.66	-	0.75	-
1464	-	0.69	-	-	-	-
1542	-	-	-	1.49	-	0.53

[a] Julian date - 2450000.
[b] P (period) in days from the index to variable stars of the Variable Star Network (VSNET) (Nogami et al. 1997)

- **Emission lines:**
  Balmer lines H$_\gamma$ (4340.46 Å), H$_\delta$ (4101.73 Å), H$_\zeta$ (3889.05 Å), Hη (3835.38 Å), and various metal lines

Metal line data from the NIST database (Fuhr et al. 1988)

		M	λ[Å]	E_u[cm^{-1}]	E_l[cm^{-1}]	A_{ul}[s^{-1}][†]
Si I		2	4102.95	39760	15394	9.6(+4)
Mn I		2	4030.75	24802	0	1.7(+7)
Mg I		1	4571.10	21870	0	2.2(+2)
		3	3829.32	47957	21850	8.9(+7)
		3	3832.35	47957	21870	6.7(+7)
		3	3838.29	47957	21911	4.5(+6)
Fe I	(B)	2	4461.65	23111	704	2.9(+4)
	(A)	2	4375.93	22846	0	2.9(+4)
	(B)	3	4216.18	23711	0	1.8(+4)
	(B)	42	4307.90	35768	12560	3.4(+7)
	(A)	42	4202.03	35768	11976	8.2(+6)
	(A)	73	3852.57	32499	17550	2.9(+6)
	(B)	828	4427.30	22997	416	3.4(+4)
Fe II		38	4583.84	44449	22637	3.8(+5)
		6F	4457.95	22810	385	2.9(-1)
		7F	4359.33	23318	385	1.1(+0)
		7F	4287.40	23318	0	1.5(+0)
		21F	4276.83	25805	2430	6.5(-1)
		21F	4243.97	25429	1872	9.0(-1)

M: multiplet number; λ: wavelength; E_u, E_l: upper and lower energy level and A_{ul}: Einstein-coefficient ([†] $x(+y) \doteq x \cdot 10^y$).

3. Line profiles

The line profiles of the variety of metal emission lines observed in the M Mira sample are presented and discussed in Richter & Wood (2001). Here we concentrate on the Fe II and [Fe II] lines in order to present some remarkable details of these lines.

Fe II and [Fe II]: All of these emission lines, namely the permitted line Fe II (M 38) and the forbidden lines [Fe II] 6F, [Fe II] 7F as well as [Fe II] 21F, appear late in phase towards the minimum light of the stars. One can roughly estimate that they must be emitted around 1.5 R$_*$ (see also Sec. 4). Therefore, these emission lines are in particular excellent diagnostic tools to investigate the dust forming zones of M Miras atmospheres.

Our observations also revealed that the Fe II and [Fe II] emission lines are not appearing during every cycle of the stars. In addition we found evidence that their erratic appearance may be because they require an exceptionally bright maximum (stronger shock waves) for excitation.

In Figs. 1 and 2 the spectral line flux F$_\lambda$ is plotted vertically, with the zero flux level for each spectrum being indicated by a tick mark. The phase of the observation is indicated (phase 0.0 corresponds to the first maximum observed). Note, that the height of the profiles is arbitrary, because we scaled them with different factors. The velocity axis corresponds to wavelength scale (λ increases to the right). Positive velocities correspond to motion outward from the center-of-mass.

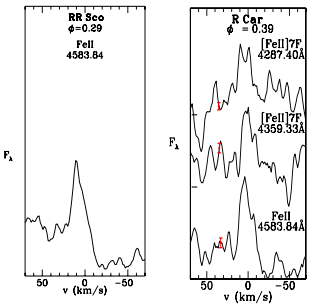

Fig. 1: **Left:** Line profile of Fe II at phase ϕ=0.29 in RR Sco (1500 μm). **Right:** Line profiles of Fe II and of the forbidden transitions [Fe II] 7F at phase ϕ=0.39 in R Car. This particular observation was taken with the 300 μm slit in poor weather conditions, so the signal to noise of these faint lines is low (σ-errorbars are indicated). Other forbidden lines were probably present but undetectable.

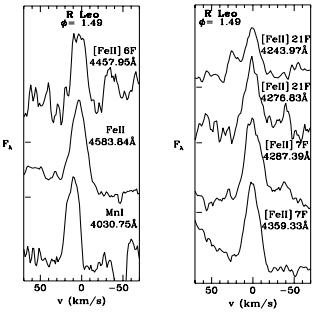

Fig. 2: **Left:** Line profiles of Mn I, Fe II and [Fe II] 6F at phase ϕ=1.49 in R Leo (1500 μm). **Right**: Line profiles of the forbidden transitions [Fe II] 7F and [Fe II] 21F at phase ϕ=1.49 in R Leo (1500 μm).

4. Fluxes

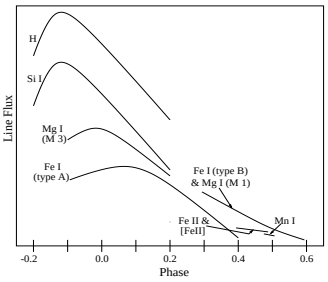

Fig. 3: Simplified time sequence for the observed emission lines and their total fluxes (in arbitary units).

Fig. 3 depicts the overall duration and flux variation with phase of emission lines in M-type Miras. Assuming a pulsation period of 1 yr and a shock velocity of 10^6 cm/s one can estimate that the shock front travels roughly 1 R_* in one period. With the assumption that the shock emerges from the photosphere (defined to be at optical depth one) at maximum $\phi = 0.0$, the radial position of the shock front r_{sh} for a given phase can be approximated: $\phi = 0.5 \propto r_{sh} = 1.5\, R_*$. Note, that because the line emission presumably originates from the post-shock material, this radius roughly corresponds to the formation region of the lines.

Fe II and [Fe II]: The permitted Fe II line and the forbidden lines [Fe II] 6F, [Fe II] 7F, and [Fe II] 21F were detected at late phases around $\phi \sim 0.3$–0.5, which correspond to a formation region of ~ 1.3–$1.5\,R_*$. These lines belong to the faintest lines observed. Additionaly one can note that the line fluxes of the [Fe II] 6F and [Fe II] 21F emission lines are weaker than the [Fe II] 7F line flux. The total line flux F_{tot} [erg cm^{-2} s^{-1}] of these lines were measured as follows:

Star	Phase	FeII (4427 Å)	[FeII] 21F (4276 Å)	[FeII] 21F (4243 Å)
RR Sco	0.29	4.7-14	-	-
R Leo	1.49	7.3-14	7.9-14	1.4-13
R Car	0.39	5.8-13:	-	-

Star	Phase	[FeII] 6F (4457 Å)	[FeII] 7F (4359 Å)	[FeII] 7F (4287 Å)
RR Sco	0.29	-	-	-
R Leo	1.49	9.0-14	1.4-13	3.0-13
R Car	0.39	-	2.5-13:	5.5-13:

Note: Numbers followed by a colon correspond to fluxes derived by normalizing to the AAVSO light curve (Mattei et al. 1980).

5. Radial velocities

Fig. 4 clearly shows that when the shock emerges from deep in the photosphere ($\phi \sim 0.0$), the post-shock emission region has a measured outward velocity of ∼10–12 km/s. As phase advances, the emission line velocity decreases until it becomes essentially zero around minimum light ($\phi \sim 0.5$). It should be noted that the material whose velocity is measured here is associated with the near-shock zone: this is quite different from the deeper, infall zone whose velocity is measured near minimum light by infrared spectra.
At first sight, it is surprising that the velocity approaches zero around minimum light. Since the lines are still in emission, the shock — which is far above the photosphere — must still be propagating outward, so that the emission lines should show a positive outward directed velocity.

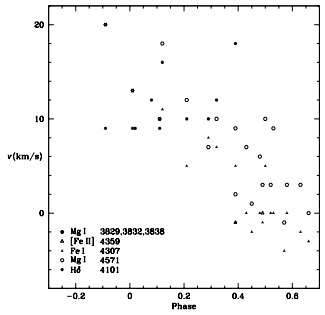

Fig. 4: The velocities (relative the stellar center-of-mass) of representative emission lines plotted against the phase of the pulsation cycle. The velocities are defined at half-height of the line profiles and are obtained from all stars in the sample.

In a simple geometric model for emission from a typical fundamental mode Mira model (e.g. see the models of Bessell et al. 1996 or Hofmann et al. 1998), the emission lines would have square profiles going from $+v_{sh}$ to -0.82×v_{sh}, where v_{sh} would be ∼5 km/s: only the emission with the most negative velocity is hidden behind the star. We would therefore expect the line emission to be centered close to velocity zero, as observed.

Fe II and [Fe II]: The velocity shifts of the forbidden lines [Fe II] 6F, [Fe II] 7F, and [Fe II] 21F as well as the permitted Fe II line were measured to be approximately 0–2 km/s.

6. Summary

A sample of six M-type Miras has been observed with a phase coverage of about one pulsation period. We obtained time-resolved, high-dispersion emission line spectra and line fluxes in the optical spectral region for the Balmer lines (Hγ, Hδ, Hζ, Hη) and for metal lines of Mg I, Mn I, Si I, Fe I, Fe II and [Fe II]. We presented details of one permitted line Fe II and five forbidden lines [Fe II], which are excellent diagnostic tools to investigate the dust forming layers of M-type Mira atmospheres. Further details on all observed lines can be gained from Richter & Wood (2001).

7. Outlook

A proper interpretation of the observations will require the help of detailed theoretical modeling. Our future work will therefore concentrate on radiative transfer calculations in moving atmospheres under conditions of non–LTE. These calculations will help to reveal the formation of the observed emission lines and to obtain the barely known thermo- and hydrodynamical conditions of the dust-forming layers of M–type Mira stars.

Acknowledgement:
This work was supported by the *Deutscher Akademischer Austauschdienst, DAAD* with a HSP III grant, project number D/99/15656 and by the *Deutsche Forschungsgemeinschaft, DFG* project number SE 420/21-1.

References

Bessell, M. S., Scholz, M., Wood, P. R.: 1996, A&A **307**, 481
Fuhr, J.R., Martin, G. A., Wiese, W. L.: 1988, J. Phys. Chem. Ref. Data **17**, Suppl.4
Hofmann, K.-H., Scholz, M., Wood, P.R.: 1998, A&A **339**, 846
Mattei, J. A., Mayer, E. H., Baldwin, M. E.: 1980, Sky Telesc. **60**, 180
Nogami D., Kato T., Baba H. et al. , 1997, Electronic Publishing, Now and the Future, Joint Discussion 12, 23rd meeting of the IAU, Kyoto, Japan
Richter, He., Woitke, P., Sedlmayr, E., Wood, P.R.: 2000, AG abstract series **17**, 61
Richter, He., Wood, P.R.: 2001, A&A **369**, 1027

Grid (1 , 1)